

# Simulation and Implementation of Decoy State Quantum Key Distribution over 60km Telecom Fiber

Yi Zhao, Bing Qi, Xiongfeng Ma, Hoi-Kwong Lo, Li Qian

Center for Quantum Information and Quantum Control

Department of Physics and Department of Electrical & Computer Engineering

University of Toronto, Toronto, Ontario, M5S 3G4, CANADA

Email: [yzhao@physics.utoronto.ca](mailto:yzhao@physics.utoronto.ca), [hklo@comm.utoronto.ca](mailto:hklo@comm.utoronto.ca)

**Abstract**—Decoy state quantum key distribution (QKD) has been proposed as a novel approach to improve dramatically both the security and the performance of practical QKD set-ups. Recently, many theoretical efforts have been made on this topic and have theoretically predicted the high performance of decoy method. However, the gap between theory and experiment remains open. In this paper, we report the first experiments on decoy state QKD, thus bridging the gap. Two protocols of decoy state QKD are implemented: one-decoy protocol over 15km of standard telecom fiber, and weak+vacuum protocol over 60km of standard telecom fiber. We implemented the decoy state method on a modified commercial QKD system. The modification we made is simply adding commercial acousto-optic modulator (AOM) on the QKD system. The AOM is used to modulate the intensity of each signal individually, thus implementing the decoy state method. As an important part of implementation, numerical simulation of our set-up is also performed. The simulation shows that standard security proofs give a zero key generation rate at the distance we perform decoy state QKD (both 15km and 60km). Therefore decoy state QKD is necessary for long distance secure communication. Our implementation shows explicitly the power and feasibility of decoy method, and brings it to our real-life.

## I. INTRODUCTION

Quantum key distribution (QKD)[1], [2] was proposed as a method of sharing a key between two parties (normally denoted by the sender Alice and receiver Bob) securely. It would be impossible for an eavesdropper to attack the QKD system without being detected. Assuming a perfect single photon source is utilized, people have proven the security of QKD based on fundamental laws of quantum physics [3], [4].

Unfortunately, in view of implementation, “perfect” devices are always very hard to build. Therefore most up-to-date QKD systems substitute the desired perfect single photon sources by heavily attenuated coherent laser sources. QKD can be performed with these laser sources over more than 120km of telecom fibers [5], [6].

However, this substitution raises some severe security concern. The output of coherent laser source obeys Poisson distribution. Thus the occasional production of multi-photon signals is inevitable no matter how heavily people attenuate the laser. Recall that the security of BB84 protocol [1] is guaranteed by quantum no-cloning theorem, the production of

multi-photon signals is fatal for the security: the eavesdropper (normally denoted by Eve) can simply keep an identical copy of what Bob possesses by blocking all single-photon signals and splitting all multi-photon signals. Most up-to-date QKD experiments have not taken this photon-number splitting (PNS) attack into account, and thus are, in principle, insecure.

Is it possible for people to develop some special measure to make QKD secure even with practical systems? The answer is yes. From physical intuition, if Alice sends out a single photon signal, and Bob luckily receives it, this bit (normally defined as in “single photon state”) should be secure, because Eve cannot split or clone it. Based on this intuition, rigorous security analysis on practical QKD system is proposed by [7] and Gottesman-Lo-Lütkenhaus-Preskill (GLLP)[8], which is based on the entanglement distillation approach to security proofs.

The main idea of GLLP’s work is not to find *which* signals are secure (i.e., single-photon signals), because it would be beyond current technology. Instead, GLLP shows that the *ratio* of secure signals can be estimated from some experimental parameters, and secure key bits can then be extracted from the raw key based on this ratio through data post-processing.

With the GLLP method the secure key generation rate, which is defined as the ratio of the length of the secure key to the total number of signals sent by Alice, is given by [8]

$$R \geq q\{-Q_\mu f(E_\mu)H_2(E_\mu) + Q_1[1 - H_2(e_1)]\}, \quad (1)$$

where  $q$  depends on the protocol; the subscript  $\mu$  is the average photon number per signal in signal states;  $Q_\mu$  and  $E_\mu$  are the gain and the quantum bit error rate (QBER) of signal states, respectively;  $Q_1$  and  $e_1$  are the gain and the error rate of the single photon state in signal states, respectively;  $f(x)$  is the bi-directional error correction rate [9]; and  $H_2(x)$  is the binary entropy function:  $H_2(x) = -x \log_2(x) - (1-x) \log_2(1-x)$ .  $Q_\mu$  and  $E_\mu$  can both be measured directly from experiments, while  $Q_1$  and  $e_1$  have to be estimated (because Alice and Bob could not measure the photon number of each pulse with current technology).

GLLP [8] has also given a method to estimate the lower bound of  $Q_1$  and the upper bound of  $e_1$ , thus giving out the

lower bound of the key rate  $R$ . However, with coherent laser sources, these bounds are not tight. It follows that the security of practical QKD set-ups can be guaranteed only at very short distance and very low key generation rate [8], [10].

A key question is thus raised: how can one extend both the maximum secure distance and key generation rate of QKD? The most intuitive choice would be to use a (nearly) perfect single photon source. Despite much experimental effort [11], reliable near-perfect single photon sources are far from practical.

Another solution to increase the maximum secure distance and key generation rate is to employ decoy states, using extra states of different average photon number to detect photon-number dependent attenuation. The decoy method was first discovered by Hwang [12]. The first rigorous security proof of decoy state QKD was presented by us [10]. It is shown that the decoy state method can be combined with standard GLLP result to achieve dramatically higher key generation rates and longer distances [10]. Moreover, practical protocols with vacua and weak coherent states as decoys were proposed [10]. Subsequently, we have analyzed the security of practical protocols [13]. Decoy method has attracted great recent interests [14].

The basic idea of decoy state QKD is as follows: Alice introduces some some “decoy” states with average photon numbers  $\nu_i$  besides the signal state with average photon number  $\mu$  ( $\neq \nu_i$ ). Each pulse sent by Alice is assigned to a state (signal state or one of the decoy states) randomly. Alice announces the state of each pulse after Bob’s acknowledgement of receipt of signals. The statistical characteristics (i.e., gain and QBER) of each state can then be analyzed separately. Note that the average photon number of certain state is only by statistical meaning, while Eve’s knowledge is limited to the actual photon number in each pulse, therefore Eve has no clue about the state of each pulse. Eve’s attack will modify the statistical characteristics (gain or QBER) of decoy states and/or signal state and will be caught. The decoy states are used only for catching an eavesdropper, but not for key generation. It has been shown [10], [13], [14] that, in theory, decoy state QKD can substantially enhance security and performance of QKD.

The power and feasibility of decoy method can be shown only by implementing it. To implement decoy state QKD, it is intuitive to utilize variable optical attenuators (VOAs) to modulate the intensity of each signal to that of its state. Actually, this is exactly the way we used.

## II. IMPLEMENTATIONS OF DECOY STATE PROTOCOLS

In [10], [13], we have proposed several protocols on decoy state QKD. The most important two protocols are the one-decoy protocol (the simplest protocol) and the weak+vacuum protocol (the optimal protocol). We have implemented both of them, over 15km (the one-decoy protocol) and 60km (the weak+vacuum protocol) standard telecom fibers.

### A. Implementation of one-decoy protocol

In one-decoy protocol, people need only *one* decoy state with average photon number per signal  $\nu < \mu$ . Alice could

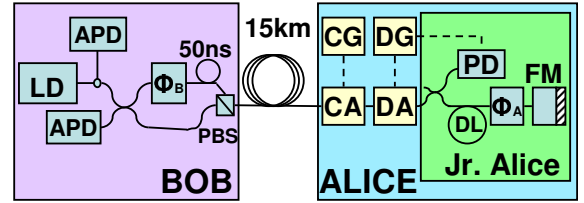


Fig. 1. Schematic of the set-up in one-decoy protocol experiment. Inside Bob/Jr. Alice: components in Bob/Alice’s package of id Quantique QKD system. Our modifications: CA: Compensating AOM; CG: Compensating Generator; DA: Decoy AOM; DG: Decoy Generator. Original QKD system: LD: laser diode; APD: avalanche photon diode;  $\Phi_i$ : phase modulator; PBS: polarization beam splitter; PD: classical photo detector; DL: Delay line; FM: Faraday mirror. Solid line: SMF28 single mode optical fiber; dashed line: electric cable.

decide the values of  $\mu$  and  $\nu$ , and the ratio of number of pulses used as decoy state to that of total pulses, then randomly assign the state to each signal by attenuating the intensity of each signal to either  $\mu$  or  $\nu$ .

We implemented the one-decoy protocol by adding acousto-optical modulators (AOMs, including CA, DA in Fig. 1) to a commercial “Plug & Play” QKD system manufactured by id Quantique (Jr. Alice and Bob in Fig. 1). We choose AOM to modulate the signals because we need this amplitude modulation to be polarization insensitive.

This QKD system is based on a 1550nm laser source with pulse repetition rate of 5MHz. Its intrinsic parameters, including dark count rate  $Y_0$ , detector error rate  $e_{detector}$ , and Bob’s quantum efficiency  $\eta_{Bob}$  are listed on Table I.

Before experiment, we perform a numerical simulation (discussed in detail in Section III) with parameters of our set-up as in Table I and optimally set  $\mu$  and  $\nu$  to 0.80 and 0.120 photons respectively. The actual distribution of the states is produced by an id Quantique Quantum Random Number Generator. Around 10% of the signals are assigned as decoy states as suggested by numerical simulation. This random pattern is generated and loaded to the Decoy Generator (DG in Fig. 1) before the experiment.

Here we describe the flow of the experiment. First, Bob generates a chain of strong laser pulses by the laser diode (LD in Fig. 1) and sends them to Alice through the 15km fiber. Second, the pulses propagate through the AOMs (CA and DA in Fig. 1, the function of CA as well as CG will be discussed in the next paragraph), whose transmittances are set maximum at this period. Third, each pulse is splitted by a coupler and part of it will be detected by a classical photo detector (PD in Fig. 1), which generates synchronizing signal to trigger

TABLE I

SOME INTRINSIC PARAMETERS OF THE QKD SYSTEM. THESE PARAMETERS ARE DIFFERENT FOR THE TWO IMPLEMENTATIONS BECAUSE THE SINGLE PHOTON DETECTORS OF THE QKD SYSTEM WERE ADJUSTED BY THE MANUFACTURER BETWEEN THE TWO EXPERIMENTS.

Implementation	$Y_0$	$e_{detector}$	$\eta_{Bob}$
One-Decoy	$2.11 \times 10^{-5}$	$8.27 \times 10^{-3}$	$2.27 \times 10^{-2}$
Weak+Vacuum	$6.14 \times 10^{-5}$	$1.38 \times 10^{-2}$	$5.82 \times 10^{-2}$

the Decoy Generator (DG in Fig. 1). Fourth, the generator holds for certain time period, during which the pulses are reflected by the faraday mirror (FM in Fig. 1) and quantum information is encoded by the phase modulator ( $\Phi_A$  in Fig. 1). Here comes the key point: fifth, the Decoy Generator (DG in Fig. 1) will drive the Decoy AOM (DA in Fig. 1) to modulate each pulse to the intensity (either 0.80 or 0.120) of the state it is assigned to exactly when the pulse propagates through the AOM. Sixth, the pulses (now in single photon level) return to Bob through the 15km fiber again. Seventh, Bob decodes the quantum information by modulating the phases of the pulses by the phase modulator ( $\Phi_B$  in Fig. 1) and see which single photon detector (APD in Fig. 1) fires.

The use of the Decoy AOM (DA in Fig. 1) shifts the frequency of the laser pulses, thus shifts the relative phase between pulses significantly. To compensate this phase shift, another AOM, the “Compensating AOM” (CA in FIG. 1) is employed to make the total phase shift multiples of  $2\pi$ . This AOM is driven by the second function generator, “Compensating Generator” (CG in FIG. 1). Its transmittance is set constant throughout the experiment.

Here we emphasize that the holding time of the Decoy Generator (DG in Fig. 1) after being triggered by the photo detector (PD in Fig. 1) must be very precise, because same modulation must be applied to the two pulses of the same signal to keep visibility high. In our experiment, the precision of this holding time is 10ns.

After the transmission of all the signals, Alice broadcasted to Bob the distribution of decoy states as well as basis information. Bob then announced which signals he had actually received in correct basis. We assume Alice and Bob announced the measurement outcomes of all decoy states as well as a subset of the signal states. From those experimental data, Alice and Bob then determined  $Q_\mu$ ,  $Q_\nu$ ,  $E_\mu$ , and  $E_\nu$ , whose values are now listed in Table II. Note that our experiment is based on BB84 [1] protocol, thus  $q = N_\mu^S/N$ , where  $N_\mu^S$  is the number of pulses used as signal state when Alice and Bob chose the same basis, and  $N = 105\text{Mbit}$  is the total number of pulses sent by Alice in this experiment.

Now we have to analyze the experimental result and estimate the lower bound of key generation rate  $R$ . This can be done by simply inputting the results in Table II to the following equations [13]:

$$Q_1 \geq Q_1^L = \frac{\mu^2 e^{-\mu}}{\mu\nu - \nu^2} (Q_\nu^L e^\nu - Q_\mu e^\mu \frac{\nu^2}{\mu^2} - E_\mu Q_\mu e^\mu \frac{\mu^2 - \nu^2}{e_0 \mu^2})$$

$$e_1 \leq e_1^U = \frac{E_\mu Q_\mu}{Q_1^L}, \quad (2)$$

in which

$$Q_\nu^L = Q_\nu (1 - \frac{u_\alpha}{\sqrt{N_\nu Q_\nu}}), \quad (3)$$

where  $N_\nu$  is the number of pulses used as decoy states, and  $e_0$  ( $=1/2$ ) is the error rate for the vacuum signal and therefore

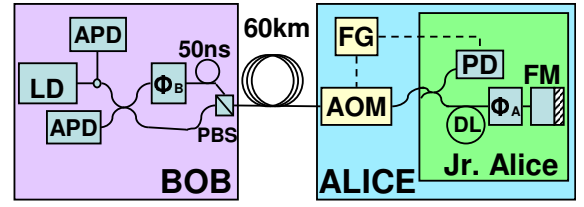


Fig. 2. Schematic of the set-up in weak+vacuum protocol experiment. Inside Bob/Jr. Alice: components in Bob/Alice’s package of id Quantique QKD system. Our modifications: AOM: Decoy AOM; FG: Functional Generator. Original QKD system: LD: laser diode; APD: avalanche photon diode;  $\Phi_i$ : phase modulator; PBS: polarization beam splitter; PD: classical photo detector; DL: Delay line; FM: faraday mirror. Solid line: SMF28 single mode optical fiber; dashed line: electric cable.

the lower bound of key generation rate is

$$R \geq R^L = q\{-Q_\mu f(E_\mu)H_2(E_\mu) + Q_1^L[1 - H_2(e_1^U)]\} \quad (4)$$

In our analysis of experimental data, we estimated  $e_1$  and  $Q_1$  very conservatively as within 10 standard deviations (i.e.,  $u_\alpha=10$ ), which promises a confidence interval for statistical fluctuations of  $1 - 1.5 \times 10^{-23}$ .

Even with our very conservative estimation of  $e_1$  and  $Q_1$ , we got a lower bound for the key generation rate  $R^L = 3.6 \times 10^{-4}$  per pulse, which means a final key length of about  $L = NR \simeq 38\text{kbit}$ . We also calculated  $R_{\text{perfect}} = 1.418 \times 10^{-3}$ , the theoretical limit from the case of infinite data size and infinite decoy states protocol, by using Eq. (1). We remark that our lower bound  $R^L$  is indeed good because it is roughly 1/4 of  $R_{\text{perfect}}$ .

### B. Implementation of weak+vacuum protocol

Weak+Vacuum protocol is similar to one-decoy protocol except that it has one more decoy state: the vacuum state, which has zero intensity. The vacuum state is to detect the background count rate. We hereby use the same notation for intensities as Subsection II-A:  $\mu$  for signal state and  $\nu < \mu$  for weak decoy state.

Weak+Vacuum protocol is theoretically predicted to have higher performance than one-decoy protocol and is optimal protocol in asymptotic case [10], [13]. Our numerical simulation (detailed discussion in Section III) shows that for our set-up (as in Table I), with data size of 105Mbit, the maximum secure distance for one-decoy protocol is 59km, while that of weak+vacuum protocol is 68km, as shown in Fig. 4. We chose 60km telecom fiber to perform weak+vacuum protocol.

The implementation of weak+vacuum protocol requires amplitude modulation of three levels:  $\mu$ ,  $\nu$  and 0. Note that it

TABLE II  
EXPERIMENTAL RESULTS IN ONE-DECOY PROTOCOL. AS REQUIRED BY GLLP [8], BIT VALUES FOR DOUBLE DETECTIONS ARE ASSIGNED RANDOMLY BY THE QUANTUM RANDOM NUMBER GENERATOR.

Para.	Value	Para.	Value	Para.	Value
$Q_\mu$	$8.757 \times 10^{-3}$	$E_\mu$	$9.536 \times 10^{-3}$	$q$	0.4478
$Q_\nu$	$1.360 \times 10^{-3}$	$E_\nu$	$2.689 \times 10^{-2}$	$f(E_\mu)$ [9]	$\leq 1.22$

would be quite hard for high-speed amplitude modulators to prepare the real “vacuum” state due to finite distinction ratio. However, if the gain of the “vacuum” state is very close (like within a few standard deviations) to the dark count rate, it would be a good approximation.

Our set-up to implement weak+vacuum protocol (Fig. 2) is very similar to that of one-decoy protocol (Fig. 1) except for the absence of the “compensating” parts (CA & CG in Fig. 1). This is because the frequency of the AOM (AOM in Fig. 2) has been precisely adjusted to the value that the phase shift caused by it is exactly multiples of  $2\pi$ . In other words, this AOM is self-compensated for our set-up.

We performed numerical simulation (as discussed in details in Section III) to find out the optimal parameters. According to simulation results, we choose the intensities as  $\mu = 0.55$ ,  $\nu = 0.152$ . Numbers of pulses used as signal state, weak decoy state and vacuum state are  $N_\mu = 0.635N$ ,  $N_\nu = 0.203N$ , and  $N_0 = 0.162N$ , respectively, where  $N = 105\text{Mbit}$  is the total data size we used.

The experimental results are shown in Table III. Note that the gain of vacuum state ( $Y_0$  in Table III) is indeed very close to the dark count rate ( $Y_0$  in Table I, third row), therefore the vacuum state in our experiment is quite “vacuum”. We could estimate the lower bound of  $Q_1$  and upper bound of  $e_1$  by plugging these experimental results into the following equations [13]:

$$\begin{aligned} Q_1 \geq Q_1^L &= \frac{\mu^2 e^{-\mu}}{\mu\nu - \nu^2} (Q_\nu^L e^\nu - Q_\mu e^\mu \frac{\nu^2}{\mu^2} - Y_0^L \frac{\mu^2 - \nu^2}{\mu^2}), \\ e_1 \leq e_1^U &= \frac{E_\mu Q_\mu - e_0 Y_0^L e^{-\mu}}{Q_1^L}, \end{aligned} \quad (5)$$

in which

$$\begin{aligned} Y_0^L &= Y_0 \left(1 - \frac{u_\alpha}{\sqrt{N_0 Y_0}}\right), \\ Y_0^U &= Y_0 \left(1 + \frac{u_\alpha}{\sqrt{N_0 Y_0}}\right), \end{aligned} \quad (6)$$

and  $Q_\nu^L$  takes the value as in Eq. (3). Again, we estimate  $Q_1$  and  $e_1$  very conservatively by setting  $u_\alpha = 10$ , which promises a confidence interval for statistical fluctuations of  $1 - 1.5 \times 10^{-23}$ .

A lower bound of the key generation rate  $R^L = 8.45 \times 10^{-5}$  per pulse is found by plugging the results of Eqs. (5) into Eq. (4), which means a final key length of about  $L = NR \simeq 9\text{kbit}$ . Note that, one-decoy protocol cannot give out a positive key rate at 60km as suggested by numerical simulation. Therefore, weak+vacuum protocol is on demand at this distance.

TABLE III

THE EXPERIMENTAL RESULTS OF WEAK+VACUUM PROTOCOL.

Para.	Value	Para.	Value
$Q_\mu$	$1.81 \times 10^{-3}$	$E_\mu$	$3.05 \times 10^{-2}$
$Q_\nu$	$5.47 \times 10^{-4}$	$E_\nu$	$7.78 \times 10^{-2}$
$Y_0$	$6.02 \times 10^{-5}$	$e_0$	0.51
$q$	0.319	$f(E_\mu)$ [9]	$\leq 1.22$

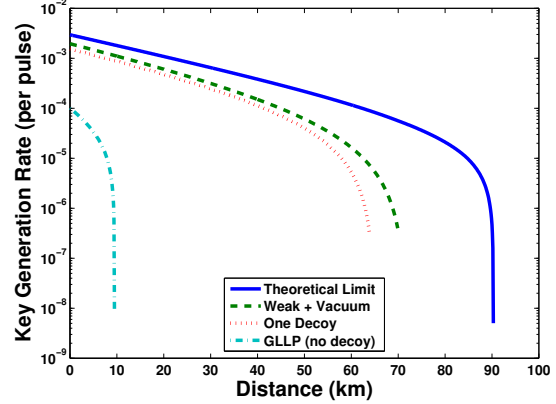


Fig. 3. Simulation result of the set-up on which we implemented the one-decoy protocol. Intrinsic parameters for this set-up is shown in the second row of Table I. Solid line: the theoretical limit of key generation rate. Its maximum transmission distance is about 90km. Dashed line: the performance of weak+vacuum protocol. Its maximum distance is about 70km. Dotted line: the performance of one-decoy protocol. Its maximum distance is about 64km. Dashed and dotted line: the performance without decoy method. Its maximum distance is only 9.5km.

### III. NUMERICAL SIMULATION

Numerical simulation is crucial for setting optimal experimental parameters and choosing the distance to perform certain decoy method protocol. Here we explain the principle of our simulation, and show some results.

The principle of numerical simulation is that for certain QKD set-up, if the intensities and percentages of signal state and decoy states are chosen, we could simulate the experimental results (gains and QBERs of all states). For example, suppose we have a QKD set-up with transmittance  $\eta$ , detector error rate  $e_{\text{detector}}$  and dark count rate  $Y_0$ , if the output intensity is set to be  $\mu$  photons per signal, the gain and QBER of this state is expected to be [15]

$$\begin{aligned} Q_\mu &= Y_0 + 1 - e^{-\eta\mu}, \\ E_\mu &= \frac{1}{Q_\mu} (e_0 Y_0 + e_{\text{detector}} (1 - e^{-\eta\mu})), \end{aligned} \quad (7)$$

respectively. With these simulated experimental outcome, we could estimate the lower bound of the key generation rate.

In experiment, it is natural to choose the intensities and percentages of signal state and decoy states which could give out the maximum key generation rate. This search for optimal parameters can be done by numerical simulation and exhaustive search. For example, we could try the values of  $\mu$  and  $\nu_i$ , the intensities of signal state and decoy states, in the range of  $[0, 1]$  with a step increase of 0.001. Similar strategy can be applied on the percentage of each state. With certain combination of intensities and percentages, the gains and QBERs of different states could be simulated by Eqs. (7), and the key generation rate can be estimated by the chosen protocol, like Eqs. (2)(3)(4) for one-decoy protocol and Eqs. (3)(4)(5)(6) for weak+vacuum protocol. We can therefore find out the optimal combination that can give maximum key generation rate.

Numerical simulation can also give the maximum secure distance for certain decoy protocol and QKD set-up. The transmittance of the system is a simple function of distance [15]  $\eta = \eta_{Bob} e^{-\alpha l}$ , where  $\alpha$  (=0.21dB/km in our set-up) is the loss coefficient. For a QKD set-up with known  $\eta_{Bob}$ ,  $\alpha$ ,  $e_{detector}$ , and  $Y_0$ , we could find out the maximum key generation rate of some protocol at distance  $l$ . The shortest distance at which the maximum key generation rate for certain protocol hits zero is defined as maximum secure distance for this protocol on this set-up. It would probably be a waste of time to perform certain decoy state protocol far beyond its maximum secure distance.

We performed numerical simulation based on the set-up on which we implemented the one-decoy protocol. The result is shown in Fig. 3. The power of decoy method is explicitly shown by the fact that the maximum distance in absence of decoy method is only 9.5km. In other words, at 15km, not even a single bit could be shared between Alice and Bob with guaranteed security. In contrast, with decoy states, our QKD set-up can be made secure over 60km, which is substantially larger than the secure distance (9.5km) without decoy states.

The set-up on which we implemented the weak+vacuum protocol is a bit different from the one we implemented the one-decoy protocol because the single photon detector had been adjusted by the manufacturer and several important properties, including  $\eta_{Bob}$ ,  $Y_0$  and  $e_{detector}$ , were changed, as shown in Table I. The simulation result for this “new” set-up is shown in Fig. 4. Clearly, the expected performance, including the key rate of certain distance and maximum secure distance of certain protocol, of this set-up is different from the previous one. This difference is natural because the properties of the system have changed.

The advantage of weak+vacuum protocol over one-decoy protocol is shown by the fact that the maximum secure distance of one-decoy protocol is 59km, which means that one-decoy protocol cannot give out a positive key rate at 60km. We confirmed this numerical simulation result by plugging experimental results  $Q_\mu$ ,  $E_\mu$ ,  $Q_\nu$  and  $q$  from Table III into Eqs. (2)(3)(4) and found indeed that key rate is not positive.

The maximum secure distance of our set-up is limited by equipment, especially the single photon detectors we used (APDs in Figs. 1&2). Given a better set-up (higher  $\eta_{Bob}$ , lower  $e_{detector}$  and  $Y_0$ ), secure decoy state QKD can be experimentally implemented over 100km, as shown in [13].

#### IV. CONCLUSION

For the first time, we have implemented decoy state QKD. We have implemented two protocols: the one-decoy protocol and the weak+vacuum protocol. Simple modifications (adding AOMs) on a commercial QKD system are made to implement decoy state QKD. The simplicity of the modification (much simpler than building a near-perfect single photon source) shows the feasibility of decoy method. Also, the high key rates and long transmission distances (60km) show the power of decoy method. Given better QKD set-ups, decoy state method could make secure QKD at even longer distances.

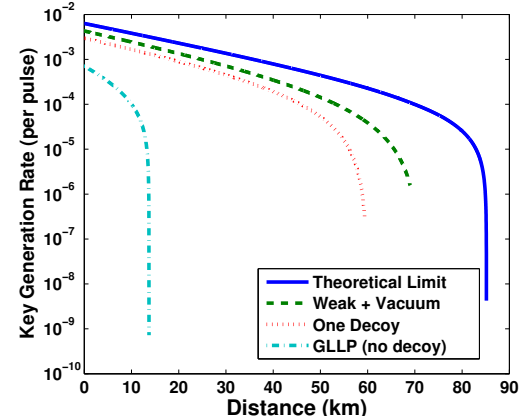


Fig. 4. Simulation result of the set-up on which we implemented the weak+vacuum protocol. The intrinsic parameters of this set-up is shown in the third row of Table I. Note that this set-up is different from the one we implemented one-decoy as reflected by the fact that in Table I, the values in row 3 are different from the values in row 2. Solid line: the theoretical limit of key generation rate. Its maximum transmission distance is about 84km. Dashed line: the performance of weak+vacuum protocol. Its maximum distance is about 68km. Dotted line: the performance of one-decoy protocol. Its maximum distance is about 59km. Dashed and dotted line: the performance without decoy method. Its maximum distance is only 14km.

We thus come to the conclusion: decoy method is ready for immediate real-life applications!

#### ACKNOWLEDGMENT

We thank generous help from many colleagues including Grégoire Ribordy. Support of the funding agencies CFI, CIPI, the CRC program, NSERC, and OIT is gratefully acknowledged.

#### REFERENCES

- [1] C. H. Bennett, G. Brassard, Proceedings of *IEEE International Conference on Computers, Systems, and Signal Processing*, (IEEE, 1984), pp. 175-179.
- [2] A. K. Ekert, *Phys. Rev. Lett.* **67** 661 (1991)
- [3] D. Mayers, *J. of ACM* **48**, 351 (2001); H.-K. Lo, H. F. Chau, *Science*, **283**, 2050 (1999); E. Biham *et al.* Proceedings of the *Thirty-Second Annual ACM Symposium on Theory of Computing (STOC'00)* (ACM Press, New York, 2000), pp. 715-724; P. W. Shor, J. Preskill, *Phys. Rev. Lett.* **85**, 441, (2000)
- [4] K. Ekert, and B. Huttner, *J. of Modern Optics* **41**, 2455 (1994); D. Deutsch *et al.*, *Phys. Rev. Lett.* **77**, 2818 (1996); Erratum: *Phys. Rev. Lett.* **80**, 2022 (1998).
- [5] C. Gobby, Z. L. Yuan, A. J. Shields, *Appl. Phys. Lett.* **84** 3762 (2004)
- [6] X. Mo, *et al.* *Opt. Lett.* **30** 2632 (2005)
- [7] H. Inamori, N. Lütkenhaus, D. Mayers, in press (available at <http://arxiv.org/abs/quant-ph/0107017>)
- [8] D. Gottesman *et al.* *Quantum Information and Computation* **4**, 325 (2004)
- [9] G. Brassard, L. Salvail, *Advances in Cryptology EUROCRYPT '93*, Vol. 765 of *Lecture Notes in Computer Science*, (Springer, Berlin, 1994), pp. 410-423.
- [10] H.-K. Lo, in *Proceedings of IEEE ISIT 2004*, p. 137; H.-K. Lo, X. Ma, K. Chen, *Phys. Rev. Lett.* **94** 230504 (2005).
- [11] J. McKeever, *et al.* *Science* **303**, 1992 (2004); Z. L. Yuan, *et al.* *Science* **295**, 102 (2002); M. Keller *et al.* *Nature* **431**, 1075 (2004)
- [12] W.-Y. Hwang, *Phys. Rev. Lett.* **91**, 057901 (2003)
- [13] X. Ma *et al.* *Phys. Rev. A* **72** 012326 (2005)
- [14] X. -B. Wang, *Phys. Rev. Lett.* **94** 230503 (2005); X. -B. Wang, *Phys. Rev. A* **72** 012322 (2005); J. W. Harrington *et al.* Arxiv: quant-ph/0503002
- [15] N. Lütkenhaus, *Phys. Rev. A* **61**, 052304 (2000).